

Integrating High-Resolution and Solid-State Magic Angle Spinning NMR Spectroscopy and a Transcriptomic Analysis of Soybean Tissues in Response to Water Deficiency

Isabel D. Coutinho,^{a*} Tiago Bueno Moraes,^a Liliane Marcia Mertz-Henning,^b Alexandre Lima Nepomuceno,^b Willian Giordani,^c Juliana Marcolino-Gomes,^b Silvia Santagneli^d and Luiz Alberto Colnago^b

ABSTRACT:

Introduction – Solid-state NMR (SSNMR) spectroscopy methods provide chemical environment and ultrastructural details that are not easily accessible by other non-destructive, high-resolution spectral techniques. High-resolution magic angle spinning (HR-MAS) has been widely used to obtain the metabolic profile of a heterogeneous sample, combining the resolution enhancement provided by MAS in SSNMR with the shimming and locking procedures in liquid-state NMR.

Objective – In this work, we explored the feasibility of using the HR-MAS and SSNMR techniques to identify metabolic changes in soybean leaves subjected to water-deficient conditions.

Methodology – Control and water-deficient soybean leaves were analysed using one-dimensional (1D) HR-MAS and SSNMR. Total RNA was extracted from the leaves for the transcriptomic analysis.

Results – The ¹H HR-MAS and CP-MAS ¹³C{¹H} spectra of soybean leaves grown with and without water deficiency stress revealed striking differences in metabolites. A total of 30 metabolites were identified, and the impact of water deficiency on the metabolite profile of soybean leaves was to induce amino acid synthesis. High expression levels of genes required for amino acid biosynthesis were highly correlated with the compounds identified by ¹H HR-MAS.

Conclusions – The integration of the ¹H HR-MAS and SSNMR spectra with the transcriptomic data provided a complete picture of the major changes in the metabolic profile of soybeans in response to water deficiency. Copyright © 2017 John Wiley & Sons, Ltd.

Additional Supporting Information may be found online in the supporting information tab for this article.

Keywords: soybean; metabolic fingerprinting; HR-MAS; SSNMR; transcriptomic

Introduction

Nuclear magnetic resonance (NMR) spectroscopy has been widely used to obtain qualitative, quantitative and structural information about organic molecules (Laghi *et al.*, 2014). As an analytical technique, NMR allows the structures of unknown metabolites to be elucidated in a non-destructive way (i.e. the analyte can be reused), and the analyses do not rely on analyte volatility, polarity, molecular weight, size, chemical structure or the sample matrix (Ramanlingam *et al.*, 2015). NMR and chromatography methods combined with mass spectrometry (MS) are the most important analytical techniques employed for metabolomics screening. Although MS produces a greater number of detectable metabolites and is more sensitive than NMR, NMR has the advantages of high reproducibility, the lack of a requirement for prior chromatographic separation, and most importantly, it requires minimal sample preparation (Emvas *et al.*, 2013).

Direct analysis by NMR is ideally suited to high-throughput metabolite profiling applications and has the advantage of detecting a wide range of metabolites in an inherently quantitative and unbiased manner. Of the magic angle spinning (MAS) techniques, solid-state NMR (SSNMR) spectroscopy methods

provide chemical environment and ultrastructural details that are not easily accessible by other non-destructive, high-resolution spectral techniques (Foston, 2014). Cross polarisation and magic angle spinning (CP-MAS) techniques have been extensively used to investigate the cell wall and protective tissues (Dick-Perez *et al.*, 2011; Serra *et al.*, 2012). In a complementary fashion, high-resolution magic angle spinning (HR-MAS) has been successfully applied to analyse the soluble metabolites in intact cells and

* Correspondence to: Isabel D. Coutinho, Embrapa Instrumentação, XV de Novembro, 1452, Centro, CEP 13560-970, São Carlos, São Carlos, Brazil. Email: isadcoutinho@hotmail.com

^a Embrapa Instrumentação, XV de Novembro, 1452, Centro, 13560-970, São Carlos, São Carlos, Brazil

^b Embrapa Soja, Rodovia Carlos João Strass, Distrito de Warta, 86001-970, Londrina, Paraná, Brazil

^c Londrina State University, Rodovia Celso Garcia Cid, Km 380, 86051-900, Londrina, Paraná, Brazil

^d Institute of Chemistry, University of São Paulo State, Rua Prof. Francisco Degni, 55, 14800-060, Araraquara, São Paulo, Brazil

tissues from many organs, such as brain, lung, kidney, heart and muscle (Oliveira *et al.*, 2014), fragile tissues (André *et al.*, 2004), and for the analysis a wide range of samples, such as fish, lamb, beef, cheese, grains, fruits and vegetables (Santos *et al.*, 2015). HR-MAS NMR combines the typical advantages of liquid-state NMR and SSNMR, such as short acquisition times for ^1H -NMR spectra, even from a few milligrams of sample. HR-MAS is a sensitive technique that is able to detect compounds with concentrations of less than 1 $\mu\text{mol/L}$ in mixtures (Santos *et al.*, 2015).

Non-destructive measurements are performed in SSNMR and HR-MAS without the need for pre-treatment extraction and separation. In addition, the signals from polar and apolar compounds are detected simultaneously, depending on the NMR pulse sequence applied. Therefore, a combination of MAS NMR techniques is very useful in studies integrating metabolic fingerprinting with transcriptomic data. Metabolic fingerprinting analyses add an important extra dimension to the information flow from DNA to RNA to protein.

Drought is the major limiting factor that affects the productivity of commercially important crops, and many efforts have attempted to improve our knowledge of plant responses to limited water conditions to improve drought tolerance. The application of MAS NMR to the study of plant metabolic responses to an abiotic stress such as drought is emerging as a promising approach (Hochberg *et al.*, 2013; Lanzinger *et al.*, 2015; Silvente *et al.*, 2012). Plants respond and adapt to environmental stress not only at a physiological and morphological level but also at the cellular and molecular level. The different mechanisms plants use to protect themselves against a water deficiency include changes in stomatal conductance mediated by the abscisic acid (ABA) hormone (Melcher *et al.*, 2009), the accumulation of osmolytes and osmoprotectant molecules (Krasensky and Jonak, 2012), and changes in the activity of antioxidant proteins (Uzilday *et al.*, 2012). These defence mechanisms involve changes in gene and protein expression, as well as alterations in metabolite abundance. In this context, a metabolic fingerprinting approach is a powerful tool to obtain an overview of the plant cellular response to stress conditions. In addition, metabolites may also serve as biomarkers for the selection of tolerant genotypes because they represent the integration of the genetic background with environmental effects (Arbona *et al.*, 2013).

Thus, in this study, we probed the feasibility of using MAS NMR techniques to identify metabolic changes in soybean leaves subjected to a water deficiency. The metabolites identified were compared with RNA-seq data (sampled under similar conditions) with the goal of integrating the transcriptomic and metabolic fingerprinting data.

Materials and methods

Chemicals and reagents

Deuterium oxide (D_2O) and TSP- d_4 (sodium salt of trimethylsilylpropionic acid) from Merck (Darmstadt, Germany) were used for the HR-MAS NMR analysis. Germitest[®] paper was used to germinate the seeds. Hoagland's solution (Hoagland and Arnon, 1950) was used for hydroponic soybean growth. Trizol[®] reagent and DNase (Invitrogen, Carlsbad, CA) were used for RNA extraction. A True-Seq kit (Illumina, San Diego, CA) was used for RNA sequencing.

Plant samples for the metabolite analysis

Soybean seeds from the Brazilian cultivar BR 16 were pre-germinated on Germitest[®] paper in a $25 \pm 2^\circ\text{C}$ growth chamber at 100% relative humidity (RH) for 96 h. Normal and homogeneous seedlings were inoculated with *Bradyrhizobium japonicum* and transferred to 1 L pots filled with substrate/sand (1:1), and the substrate contained soil/sand/organic compounds (3:2:2). The pots were stored in a glasshouse at $28 \pm 2^\circ\text{C}$, and the temperature and RH were recorded every 5 min with a thermohygrograph (HOBO U14-002, Onset[®], Bourne, MA). A completely randomised experimental design was employed, with two treatments (water deficiency – WD; control – C), and 15 replicates.

The plants were grown under optimal irrigation conditions until the V3 stage (Fehr *et al.*, 1971). One day before the water deficiency was induced (at the end of the afternoon), all pots were saturated with water and the excess water was allowed to drain overnight. On the following morning, the pots were wrapped in polyethylene bags and the central region of the pots was covered with cotton around the stem base to prevent water loss by evaporation, as described by Ferreira *et al.* (2015). The control plants were well hydrated, whereas irrigation was withheld from the water deficiency group. Stomatal conductance (Gs) was monitored daily with a portable infrared gas analyser (LI-6400XT, LI-COR) by sampling the central leaflet of the third fully expanded trifoliate leaf (apex-base direction). When the water deficiency plants showed Gs values less than 200 $\text{mmol H}_2\text{O/m}^2/\text{s}$, which corresponds to moderate drought stress (Flexas *et al.*, 2004; Rodrigues *et al.*, 2012), the photosynthetic rate (A), sub-stomatal CO_2 (Ci) and stomatal conductance (Gs) were also measured on the central leaflet of the third fully expanded trifoliate leaf (apex-base direction) via the portable infrared gas analyser (LI-6400XT, LI-COR). Measurements were collected in the glasshouse from 9 h at 1000 $\mu\text{mol/m}^2/\text{s}$ photosynthetically active radiation (PAR), with a CO_2 reference of 400 $\mu\text{mol/mol}$, a water reference ranging from 18 to 20 mmol/mol , and a CO_2 flux of 400 $\mu\text{mol/s}$. The same trifoliate leaf was subsequently sampled, wrapped in aluminium foil, immediately immersed in liquid nitrogen, and then stored at -80°C until the metabolite analysis. Prior to the metabolic analysis, the samples were lyophilised and milled.

Metabolic analysis

High-resolution magic angle spinning (HR-MAS). Eight milligrams of soybean leaves were suspended in 40 μL of D_2O containing 0.01% w/v TSP- d_4 , mixed using a bench top whirlimix for 15 s and centrifuged for 5 min. The samples were loaded into zirconium HR-MAS rotors and sealed. ^1H HR-MAS spectroscopy was performed at 14.1 T (600 MHz for ^1H observation) at a temperature of 25°C using an Advance 600 Bruker NMR spectrometer equipped with a PH HR-MAS 600 S3 HCD 4 mm probe and a 5 kHz spinning rate.

Three different pulse sequences were evaluated. Two were a common Carr–Purcell–Meiboom–Gill (CPMG) spin-echo train and a CPMG sequence with suppression of J-modulation (PROJECT) by 90_y refocusing pulses (Aguillar *et al.*, 2012). The CPMG sequences used a T2 filter to suppress the broad signals from macromolecules. Arrays of variables τ (echo time, τ : 90, 95, 110, 120, 140 and 160 μs) and n (loop cycles, n : 4–50) were studied to permit broad signal attenuation and to optimise the suppression of the macromolecule signals. The one-dimensional (1D) nuclear Overhauser effect spectroscopy (NOESY) pulse sequence without

a T2 filter was also evaluated. For the three NMR pulse sequences, the spectra were acquired with a 4.6 s presaturation pulse, an acquisition time of 2.72 s (64 k points) and an accumulation of 128 transients. The free induction decays (FIDs) were automatically Fourier-transformed after the application of an exponential window function with a line broadening of 1.0 Hz. Phasing and baseline corrections were performed within TopSpin software. The ^1H -NMR MAS spectra of soybean leaves were assigned using the following identification strategies: (i) the ^1H -NMR spectra were queried on public databases (Human Metabolome Database – HMDB, and well established NMR Suite Professional version evaluate 8.1, Chenomx); (ii) the annotations were confirmed with two-dimensional (2D) NMR spectra (correlation spectroscopy (COSY), heteronuclear single quantum correlation (HSQC) and 2D J-Resolved) of soybean leaf extracts.

SSNMR. The experiments were performed on an Avance III 400 WB HD SSNMR spectrometer operating at 9.4 T using a commercial double resonance of 4 mm. Typical spinning speeds were 10.0 kHz. The lyophilised soybean leaves were packed in 4 mm zirconia rotors. Rigid and semi-rigid molecules were analysed using ^{13}C $\{^1\text{H}\}$ CP-MAS experiments. Spectra were acquired using a spectral width of 500 kHz, an acquisition time of 20 ms, a ^1H pulse length of 3.3 μs , a contact time of 1.5 ms (a linear ramp on the ^1H contact pulse with a 30% slope) and a recycling delay of 3 s. Mobile molecules were analysed using single pulse excitation (SPE) techniques due to the short longitudinal relaxation times (T_1 values) of these components. For the SPE-MAS experiments, ^{13}C $\{^1\text{H}\}$ MAS spectra were acquired using a spectral width of 500 kHz, an acquisition time of 20 ms and a recycling delay of 20 s. All spectra were acquired under TPPM-15 proton decoupling during the data acquisition by applying decoupling pulses of 5.8 μs . ^1H -MAS spectra were acquired using a pulse sequence with an incorporated T2 filter (spin echo) and an exchange block of $t = 1$ ms. The chemical shifts were reported relative to tetramethylsilane (TMS).

Data analysis. The ^1H -NMR data were reduced to ASCII files in a range between 0.00 and 10.00 ppm. The spectra data was reduced to ASCII files using the Bruker TopSpin 3.5. Each dataset have been arranged in a $X_{(I,J)}$ matrix, where I corresponded to the samples, 18, and J corresponded to columns of 32 K variables. The region corresponding to residual signal of water and TSP was excluded. The data preprocessing and partial least squares discriminant analysis (PLS-DA) from ^1H -NMR were performed using Matlab R2016b and PLS-Toolbox.

Transcriptomic analysis

RNA-seq analysis. Soybean seeds from the BR 16 cultivar were pre-germinated on Germitest® paper in a $25 \pm 1^\circ\text{C}$ growth chamber at 100% RH for 96 h. The seedlings were placed in 36 L boxes containing 50% Hoagland's solution (Hoagland and Arnon, 1950) and continuously aerated. The nutrient solution was replaced weekly, as described by Rodrigues *et al.* (2012). The plants were allowed to grow in a glasshouse under optimal developmental conditions until the V4 stage (Fehr *et al.*, 1971). Water deficiency stress was applied by removing the plants from the hydroponic solution and exposing them to ambient air in boxes without the nutrient solution for up to 150 min. Leaves and roots from three biological replicates (each one comprised a 10 plant pool) were sampled at six time points: 0, 25, 50, 75, 100,

125 and 150 min after exposure to ambient air. The samples were immediately frozen in liquid nitrogen and stored at -80°C .

Total RNA was extracted from the leaves with Trizol® Reagent according to the manufacturer's instructions (Invitrogen) and treated with DNase (Invitrogen). After RNA quality and integrity were analysed, equimolar quantities of the purified total RNA samples were pooled to produce the WD 1 (25 min + 50 min); WD 2 (75 min + 100 min) and WD 3 (125 min + 150 min) libraries for each of the three replicates. The non-stressed samples were used to produce the control libraries. The samples were prepared for sequencing using the True-Seq kit (Illumina). The libraries were distributed into five lanes on a flow cell for sequencing in a Hi-Seq 2000 instrument (Illumina). The raw data were uploaded to the GeneSifter database (Geospiza, Seattle, WA) for alignment with a reference genome. Base calling of the raw data was performed by parsing the reads according to their respective barcodes and trimming to remove adaptors and primer sequences. Output sequences were aligned with the soybean genome (Schmutz *et al.*, 2010) (Glyma v1.1 from the Soybase database [<http://www.soybase.org>]) using the Burroughs-Wheeler alignment (BWA) method (Li and Durbin, 2009). For an additional alignment, a post-processing toolset (Picard; <http://broadinstitute.github.io/picard/>) was used for local realignment, duplicate marking, and score recalibration to generate a final aligned set of genomic reads. Because mapping included both unique and multiple reads, we counted these two types differently. Unique reads were counted as a whole count, whereas multiple reads were counted proportionally for each location to which they were mapped (up to five sites) when none of the adjacent unique reads were observed. Multiple reads that mapped next to a set of unique reads mapped to one location were fully counted at that site. Based on this alignment, sequences were mapped to exons, introns, and intergenic regions, which were characterised as sequences outside of any annotated gene. The remaining unmapped reads were then aligned to a spliced reference created using all possible combinations of known exons to generate putative splice junction sites based on the annotation method described earlier. These aligned data were then used to calculate the gene expression levels using the total exon and known splice reads for each annotated gene to generate a count value per gene. For each library, a normalised expression value was calculated for each gene using the reads per mapped million (RPM), which was calculated by dividing the count value by the number of millions of mapped reads. The levels of the differentially expressed genes were calculated for the three different levels of water deficiency (WD 1, WD 2 and WD 3) by comparing the water deficiency stress libraries to the control libraries at each time-point, and generating fold change values. These expression values are presented as log₂ ratios of the fold changes, with a cutoff of 2.

The key enzymes involved in the biosynthesis of water deficiency-responsive metabolic compounds detected by the NMR analysis were identified from the KEGG database (Kyoto Encyclopaedia of Genes and Genomes – <http://www.genome.jp/kegg/>). The sequences of the genes were obtained from the NCBI (<http://www.ncbi.nlm.nih.gov/>), Soykb (<http://soykb.org/>) and Phytozome (<https://phytozome.jgi.doe.gov/pz/portal.html>) databases.

MapMan analysis. MapMan 3.6.0RC1 software (Thimm *et al.*, 2004) was used to provide a complete picture of the major changes in the transcriptome profile of soybeans subjected to a water deficiency, allowing the interaction between the transcriptomic and the NMR metabolic data. *Glycine max* Mapping

was downloaded from the MapMan Store (<http://mapman.gabipd.org/web/guest/mapmanstore>) (Usadel *et al.*, 2009) and formatted according to the manufacturer's instructions. The gene expression values corresponded to the log₂ ratio of the fold changes obtained from the three different levels of water deficiency (WD 1, WD 2 and WD 3) and were calculated as described earlier.

Results and discussion

Physiological measurements in the plants used for the metabolite analysis

The physiological features of BR 16 soybean plants subjected to drought stress and control conditions were evaluated during the experiment to monitor the water deficiency treatment in the plants used for the metabolite analysis. Figure 1 shows the photosynthetic rate, stomatal conductance, intercellular CO₂ concentration and transpiration rate on the fourth day after irrigation was stopped. Based on these data, the water deficiency treatment was effective because the plants' physiological characteristics were significantly altered by the water deficiency stress, as described in previous studies (Flexas *et al.*, 2004; Rodrigues *et al.*, 2012; Rodrigues *et al.*, 2015). For example, the photosynthetic rate [Fig. 1(A)] was strongly inhibited in response to water deficiency, in part as a consequence of the low stomatal conductance [Fig. 1(B)], which decreased from 0.7 to 0.01 mm H₂O/m²/s in the control vs. stressed plants, respectively. A similar decrease was observed for the transpiration rate [Fig. 1(C)], which declined from 4.84 to 0.38 (mm/m²/s) in the control and water deficiency treatments, respectively. However, the intercellular

CO₂ concentration [Fig. 1(D)] increased in the water deficiency plants compared to the control plants, suggesting a decrease in the ability of the mesophyll chloroplasts to fix the available CO₂.

Metabolic analysis

HR-MAS NMR analyses. The spectrum obtained with a 1D NOESY pulse sequence [Fig. 2(C)] shows the broad signals of macromolecules or molecular assemblies, which have a short transverse relaxation time (T₂), in addition to a sharp line of the small metabolites. The broad lines were suppressed with T₂ filters using a convectonal CPMG pulse sequence [Fig. 2(A)]. However, the best spectrum was obtained with the PROJECT sequences [Fig. 2(B)] using the anomeric proton from glucose at δ 5.22 [Fig. 2(C)] as a reference. The CPMG spectrum showed J-modulation distortions that were not observed in the PROJECT spectrum. The PROJECT sequences [-90°-(τ -180°- τ -90°- τ -180°- τ)-FID] use a perfect echo approach, or J-Refocusing method, to minimise signal dephasing, which becomes substantial in high fields, even at short echo times (Aguilar *et al.*, 2012). The echo times from the PROJECT pulse sequence were the next parameters to be optimised. Optimisation of this parameter is required to suppress the macromolecule and lipid signals and enhance the small molecule signals. In this context, we evaluated different echo times (τ) in the CPMG pulse sequence. The broad signals were reduced from 0.90 ms of echo time, whereas the higher τ values decreased the signal-to-noise ratio as expected. Intermediate τ values between 1.00–0.90 ms showed macromolecule signals appropriate to the filter. Thus, a τ value of 0.95 ms was used for acquisition because it had the best signal-to-noise ratio.

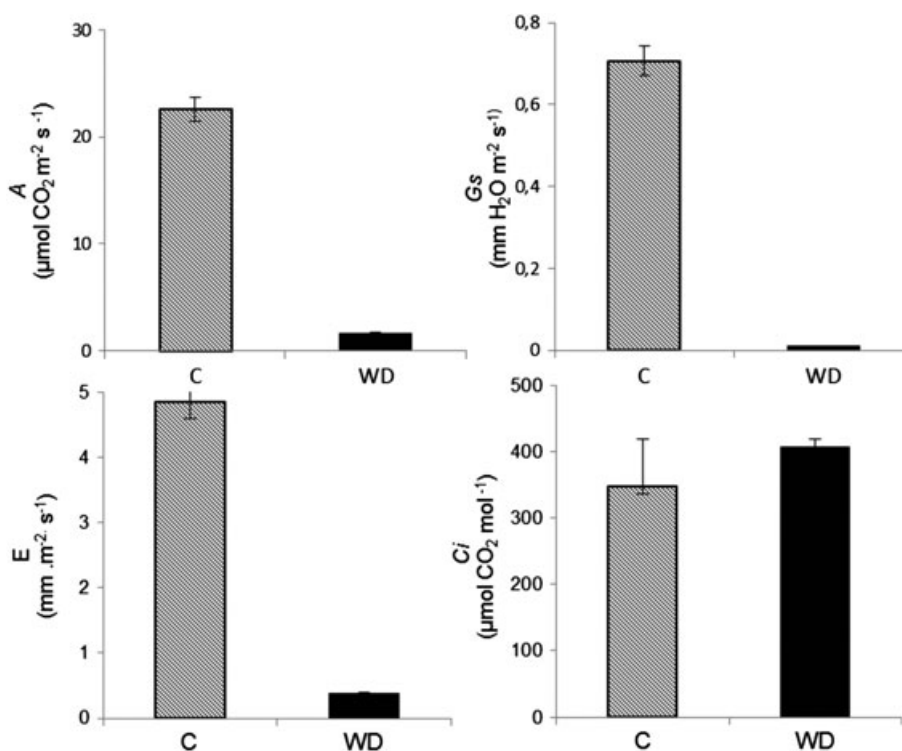


Figure 1. Physiological parameters measured on well irrigated (C, control) and drought-stressed (WD, water deficiency) soybean plants. (A) Photosynthetic rate (A , in mol CO₂/m²/s), (B) stomatal conductance (G_s , in mol H₂O/m²/s), (C) transpiration rate (E , in mmol H₂O/m²/s) and (D) intercellular CO₂ concentration (C_i , in mol CO₂/mol) were measured with a LiCor Portable Photosynthesis System. The (\pm) standard error bars are shown.

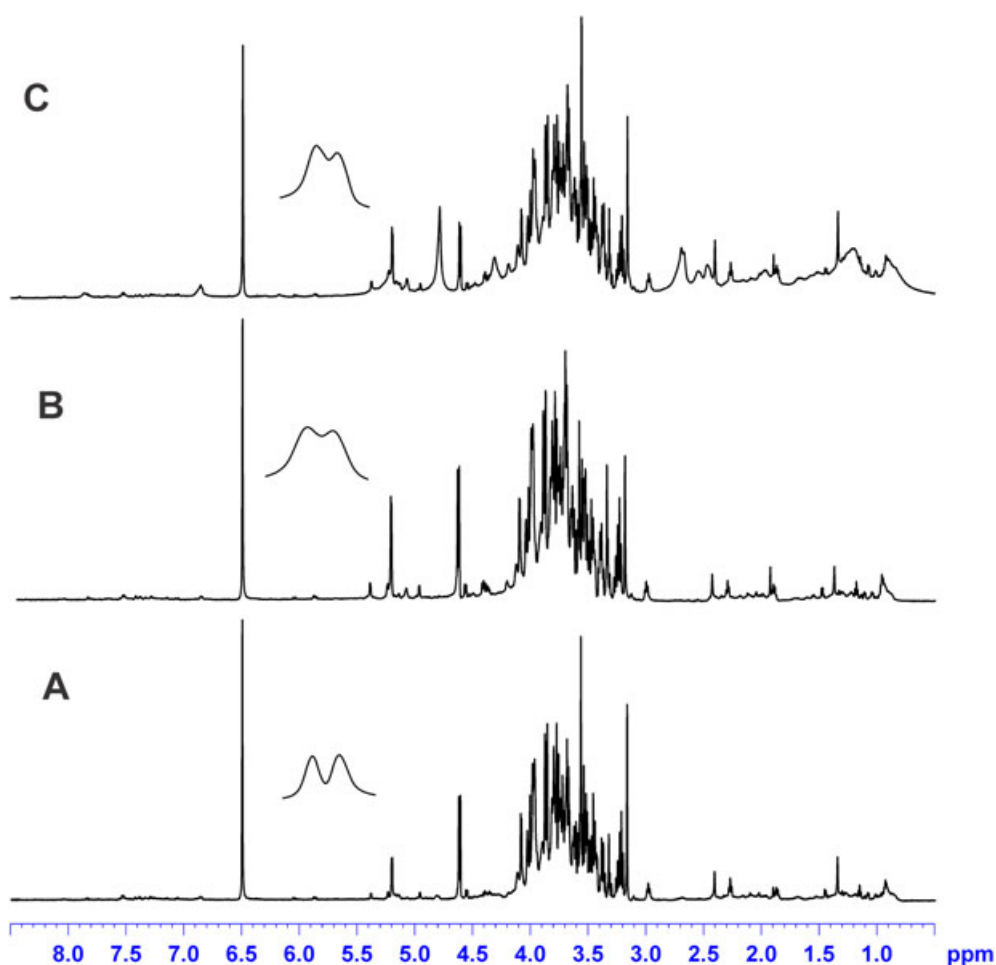


Figure 2. The effect of J-modulation distortions in CPMG spectra compare to PROJECT and 1D NOESY (without T2 filter). The highlighted signal corresponding to glucose signal. (A) 1D NOESY, signal-to-noise ratio 2.75; (B) PROJECT, signal-to-noise ratio 7.96; (C) CPMG signal-to-noise ratio 5.23. [Colour figure can be viewed at wileyonlinelibrary.com]

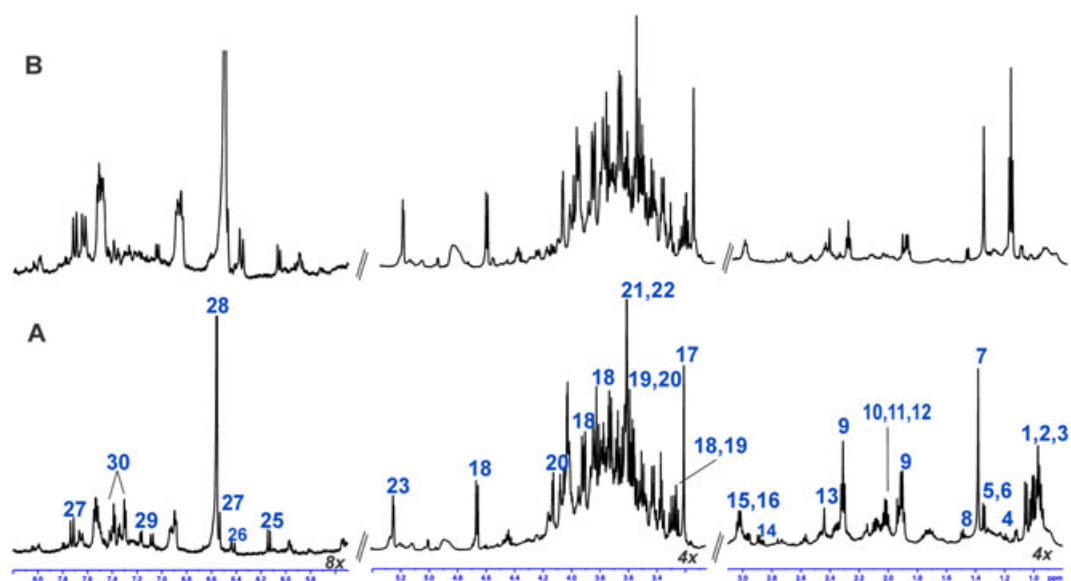


Figure 3. ^1H HR-MAS NMR spectrum of lyophilised soybeans upon control and water deficiency conditions using PROJECT pulse sequence: (A) water deficiency sample; (B) control sample. [Colour figure can be viewed at wileyonlinelibrary.com]

Table 1. Chemical shifts (δ) and coupling constants (Hz) of the metabolites identified from soybean leaves

Metabolites	δ ^1H (multiplicity, J Hz)
Isoleucine (1)	0.97 (m), 1.40 (m)
Leucine (2)	0.97 (t, 6.2), 1.70 (m)
Valine (3)	0.99 (d, 7.0), 2.27 (m)
Ethanol (4)	1.18 (t, 7.3)
Lactate (5)	1.33 (d, 6.6)
Threonine (6)	1.33 (d, 7.3)
Hydroxy-isobutyrate (7)	1.35 (s)
Alanine (8)	1.48 (d, 7.3)
GABA (9)	1.90 (q, 7.6), 2.29 (t, 7.4, 7.5), 3.03 (t, 7.5)
Acetic acid (10)	1.92 (s)
Glutamate (11)	2.01 (m), 2.08 (m)
Proline (12)	2.07 (m), 2.35 (m)
Succinic acid (13)	2.44 (s)
Asparagine (14)	2.86 (dd, 7.9, 16.6), 2.96 (dd, 4.2, 12.2)
Malonic acid (15)	3.11 (s)
Lysine (16)	3.03 (t, 7.5)
Choline (17)	3.20 (s)
β -Glucose (18)	4.65 (d, 8.1)
Betaine (19)	3.25 (s), 3.88 (s)
Fructose (20)	4.12 (dd, 2.7, 10.0)
Glycine (21)	3.59 (s)
Pinitol (22)	3.60 (s)
α -Glucose (23)	5.15 (d, 3.7)
Sucrose (24)	5.42 (d, 3.6)
<i>cis p</i> -Coumaric acid (25)	7.58 (d, 8.6), 6.87 (d, 8.6), 7.07 (d, 12.3), 6.06 (d, 12.3)
<i>trans p</i> -Ferulic acid (26)	6.50 (d, 16.0), 6.93 (d, 8.2), 7.16 (dd, 8.3, 2.0), 7.23 (d, 2.0), 7.72 (d, 16.0)
<i>trans p</i> -Coumaric acid (27)	7.61 (d, 8.5), 6.92 (d, 8.5), 6.37 (d, 16.0), 7.65 (d, 16.0)
Fumaric acid (28)	6.47 (s)
Tyrosine (29)	6.89 (d, 8.9), 7.20 (d, 8.8)
Phenylalanine (30)	3.10 (d, 8.2), 7.38 (m)

Metabolite identification using ^1H -HR-MAS and metabolic changes induced by a water deficiency. The ^1H -HR-MAS spectra of soybean leaves under water deficiency and control conditions were acquired with a PROJECT pulse sequence and are shown in Fig. 3. The signals of 30 metabolites in the soybean leaf spectra (Table 1) were assigned using the corresponding diagnostic ^1H -NMR signals and coupling constants. The amino acids identified were isoleucine (1) δ 0.97 (m), leucine (2) δ 1.70 (m), valine (3) δ 0.99 of 6H (d, 7.0), threonine (6) δ 1.33 of 3H (d, 7.6), alanine (8) δ 1.48 of 3H (d, 7.3), GABA (9) δ 1.90 3H (q, 7.4), δ 2.29 of 2H (t, 7.5), δ 3.03 of 2H (t, 7.5), glutamate (10) δ 2.01 of 3H (m), δ 2.08 of 3H (m), proline (12) δ 2.07 (m), δ 2.35 (m), asparagine (14) δ 2.86 of 2H (dd, 7.9, 16.6), δ 2.96 of 2H (d, 4.2, 12.2), lysine (16) δ 3.03 of 3H (t, 7.5), tyrosine (29) δ 6.86 of 2H (d, 8.9), δ 7.20 of 2H (d, 8.8) and phenylalanine (30) δ 3.10 of 2H (d, 8.2), δ 7.38 5H (m). Ethanol (4), lactate (5), hydroxy-isobutyrate (7), acetic acid (10), succinic acid (13), malonic acid (15), choline (17), betaine (19) and fumaric acid (28) were assigned using the signals at 1.18 (t, 7.3), 1.33 (d, 6.6), 1.35 (s), 1.92 (s), 2.44 (s), 3.11 (s), 3.20 (s), 3.25 (s), 3.60 (s) and 6.47 (s) ppm, respectively. β -Glucose (18) and α -glucose (23) were identified using the characteristic signals of the anomeric protons at 4.65 (d, 8.1) and 5.15 (d, 3.7). Fructose (20) was assigned using the signal at δ 3.99 (dd, 2.7, 10.0). The minor signals at δ 6–10 were attributed to hydroxycinnamic acid derivatives. The characteristic signals of hydroxycinnamic acid were detected as pairs of doublets at δ 6.06/7.07 and 6.37/7.65, corresponding to *cis p*-coumaric acid (25) and *trans p*-coumaric acid (27), and 6.50/7.72, corresponding to *trans p*-ferulic acid (26), due to coupling of the olefinic protons with Z (*trans*, $J = 16.0$ Hz) and E (*cis*, $J = 12.0$ Hz) configurations. The COSY experiment (Supporting Information Fig. S10) was useful for confirming the presence of signals from a pair of olefinic hydrogens from *trans-p*-coumaric acid (27) that overlapped with the intense signal of fumaric acid (δ 6.53 s). The 2D J Resolved experiment was proper to accurate assignment of signals corresponding to amino acids, mainly, at δ 0.90–2.60 (Fig. S11).

The spectra of drought-stressed, lyophilised soybean leaves [Fig. 3(A)] revealed striking differences from those of control leaves [Fig. 3(B)]. In applying PLS-DA to ^1H -NMR data, differences were observed between the treatment. As seen in Fig. 4 (A), there is a clear discrimination possible between the control and stress samples. This separation took place in the first two latent variables,

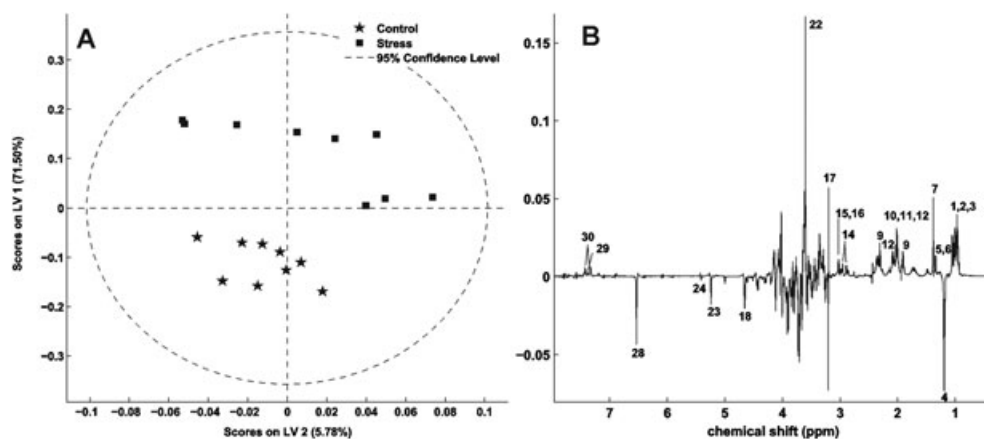


Figure 4. Partial least squares discriminant analysis (PLS-DA) based on ^1H HR-MAS NMR spectrum of lyophilised soybeans. (A) Scores plot LV1 \times LV2; (B) LV1 loadings plot shows metabolites 1, 2, 3, 6, 7, 9, 10, 11, 12, 14, 15, 16, 17, 22, 29 and 30 are up-regulated in response to water deficiency, while the metabolites 4, 18, 23, 24 and 28 are down-regulated.

which cumulatively account for 77.28% of explained variation. The impact of water deficiency on the metabolite profile of soybean leaves was to induce the biosynthesis of several amino acids, including isoleucine (1), leucine (2), valine (3), threonine (6), GABA (9), glutamate (11), proline (12), asparagine (14), tyrosine (29) and phenylalanine (30), which were not detected in control plants [Fig 4(B)]. In addition, the metabolites 7, 9, 10, 15, 16, 17 and 22 are up-regulated in response to water deficiency, while the metabolites 4, 18, 23, 24 and 28 are down-regulated. Different results were obtained by Silvente *et al.* (2012), who studied the metabolic response of two soybean genotypes with different drought stress tolerances and showed that the free amino acid content decreased in the leaves from both genotypes in response to drought. Moreover, the GABA levels were significantly decreased in the leaves of the tolerant cultivar but not in the leaves of the sensitive cultivar (Silvente *et al.*, 2012). Based on our data, the GABA (9) levels increased in BR 16 soybean leaves, which is considered a sensitive genotype, in response to drought (Fig. 3). Thus, the differences in the GABA level may distinguish drought-sensitive and drought-tolerant cultivars.

Proline is considered to act as an osmolyte, reactive oxygen species (ROS) scavenger and molecular chaperone that stabilises protein structure, and accumulates in many plant species in response to different environmental stresses, including water deficiency (Verslues and Sharma, 2010; Krasensky and Jonak, 2012). Branched chain amino acids such as isoleucine (1), leucine (2), and valine (3) have also been reported to act as osmolytes (Bowne *et al.*, 2012). In grapevine, the accumulation of proline and branched chain amino acids (proline, valine, leucine, threonine and tryptophan) was correlated with water deficiency-driven changes in the leaf water potential (Hochberg *et al.*, 2013). Additionally, recent studies of drought-stressed barley grain indicated that the free amino acid levels increased only in the sensitive cultivars (Lanzinger *et al.*, 2015). Our data revealed the biosynthesis/accumulation of both proline and free amino acids in response to drought stress, indicating that mechanisms involved in ROS scavenging and osmotic adjustment were activated in the drought-sensitive soybean cultivar BR 16 (Fig. 3). Consistent with this observation, we also identified the differential expression of several peroxidase-coding genes (Figs S3 and S4).

The ^1H HR-MAS NMR analysis also showed an increase in the phenylalanine levels, consistent with a previous analysis of the metabolites in drought-stressed grapevine, in which the phenylalanine levels decreased at the beginning of water deficiency stress but accumulated on day 34 of water deficiency, indicating the importance of this amino acid in long-term responses to drought stress (Hochberg *et al.*, 2013). Metabolic differences between short-term (six days) and long-term (18 days) drought stress have been reported. For example, in the C4 perennial grass species Bermuda grass, short-term stress did not change the contents of most amino acids (except for methionine, serine, GABA, isoleucine and mannose), whereas long-term stress led to the accumulation of most of the metabolites detected, including proline, asparagine, phenylalanine, methionine, serine, 5-hydroxyornithine, GABA, glycine, threonine and valine (Du *et al.*, 2012).

Unexpectedly, drought stress resulted in lower ethanol levels (4). Although the mechanism by which ethanol decrease in response to drought stress has not been determined, a previous study reported ethanol production and accumulation in aerial tissues of severely stressed conifer seedlings, which was believed to be associated with heat injury (e.g. membrane damage) due

to a reduction in transpirational cooling after stomatal closure and drought-induced hypoxia (Manter and Kelsey, 2008). Our physiological analysis showed a decrease in stomatal conductance [Fig. 1(B)], which may have caused a reduction in transpirational cooling and oxygen disposal (hypoxia), leading to ethanol accumulation. Based on the results and discussion described earlier, HR-MAS is a versatile and sensitive probe for the investigation of the metabolite profiles of tissues under abiotic stress, without the necessity for pre-treatment extraction and separation.

SSNMR and changes in polysaccharide metabolism induced by water deficiency.

The SSNMR experiments were performed to detect compositional differences and to distinguish differences in the molecular mobility of various polysaccharide constituents in soybeans grown under water deficiency and control conditions. Figure 5(A) shows the CP-MAS $^{13}\text{C}\{^1\text{H}\}$ spectra of lyophilised drought-stressed and control soybean leaves normalised to the intensity of the peaks at δ 72. Spectral regions were assigned based on data in the literature (Dick-Perez *et al.*, 2011; Hatcher, 1987; Knicker & Lüdemann, 1995; Lemma *et al.*, 2007; Carvalho *et al.*, 2009; Conte *et al.*, 2010; Iulianelli and Tavares, 2016). Six different chemical shift ranges were clearly observed (Fig. 5) in both spectra. The first region (δ 0–40) was assigned to glycoprotein side chains. The signal from δ 50–65 was attributed to O-alkyl groups, such as the methoxy groups present in lignin-like structures, C6 of saccharides, and the N-alkyl groups of amino acids. The signals from δ 60–90 were assigned to C1 to C5 in carbohydrates (cellulose and hemicellulose). The strong signal at δ 72 was assigned to carbons C2, C3 and C5 of carbohydrates and the signal at δ 83 to C4 was assigned to amorphous cellulose, hemicellulose and cellulose.

The signals from δ 90–115 were assigned to the acetal carbons in the xylene systems of hemicellulose (δ 101) and to C1 of the cellobiose units in cellulose I (δ 105). The signals from δ 120–140 were assigned to the aromatic carbons of lignin and proteins. The region between δ 165 and 180 was assigned to the acyl functional groups (C = O) of aliphatic carboxyl acids, esters and the amide groups of proteins (δ 173).

Therefore, the major difference between the CP-MAS spectra of drought-stressed and control lyophilised soybean leaves was a slight increase in the signal corresponding to glycoproteins, hemicellulose, cellulose and the amide groups of proteins in soybeans subjected to the water deficiency treatment. According to several studies, cellulose biosynthesis is increased or decreased in response to water deficiency; however, these changes depend on the species. Increased cellulose biosynthesis is a mechanism by which cell wall integrity and cell turgor pressure are maintained, thus allowing continuous cell growth at a low water potential (Gall *et al.*, 2015).

A CP-MAS NMR sequence is appropriate for the investigation of a compound with strong dipolar interactions, which is normally observed in materials with limited mobility in a solid, such as proteins and carbohydrates. The samples were also analysed with ^{13}C SPE-MAS. This sequence enhances the signals of mobile compounds (lipids and the mobile parts of proteins and carbohydrates) in relation to the immobile compounds (proteins and carbohydrates). Therefore, SPE spectra exhibit several sharp signals between δ 10 and 45, corresponding to fatty acid methyl and methylene groups, and from δ 120 and 130 (the carbons fatty acids double bonds). The broad lines in the SPE spectra at δ 50–90 were assigned to carbohydrates in the solid state. A slight

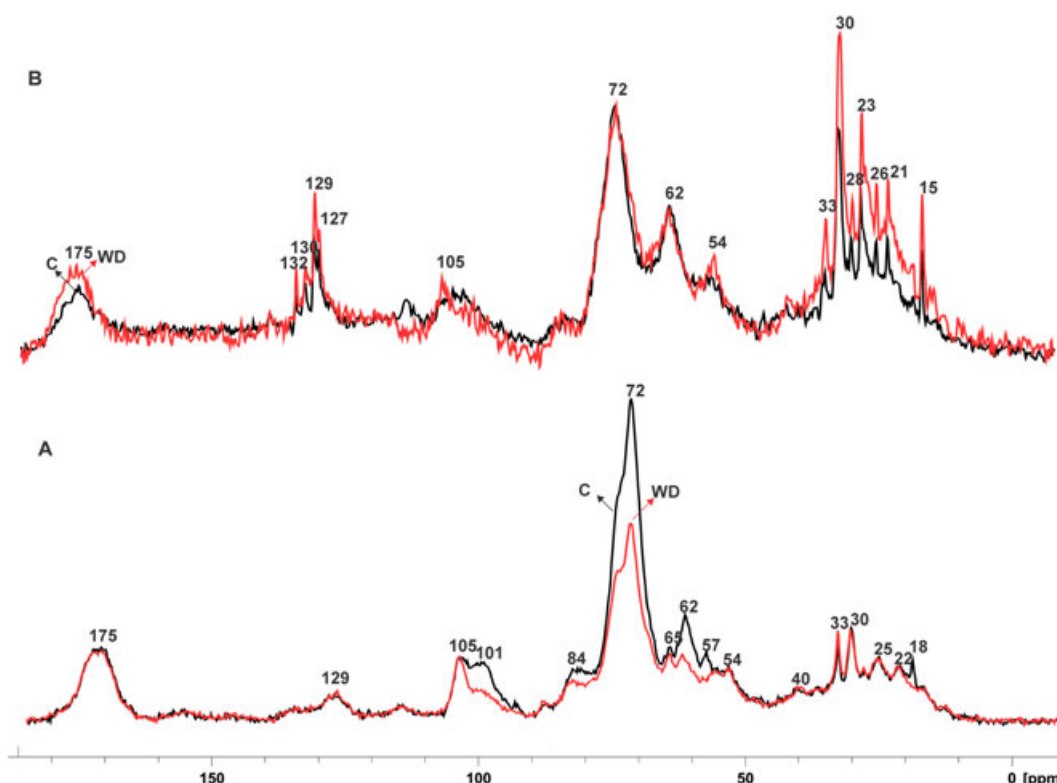


Figure 5. (A) ^{13}C CP-MAS of lyophilised soybean leaves under water deficiency (red) and control (black) conditions. (B) ^{13}C SPE-MAS of lyophilised soybean leaves under water deficit (red) and control (black) conditions. [Colour figure can be viewed at wileyonlinelibrary.com]

difference was observed between the SPE-MAS spectra of drought-stressed and control soybeans, mainly due to signals corresponding to mobile fatty acids (10 and 45 ppm). The presence of unsaturated fatty acids was confirmed in the ^1H -SPE-MAS spectra (Fig. 6). These spectra showed a typical unsaturated fatty acid signal with peaks at δ 0.95, 1.33, 2.08, and 2.81, corresponding to the methyl and methylene groups, and the peak at 5.34 ppm was assigned to ^1H in the unsaturated bonds. The spectra did not show a signal at δ 4.2, indicating the absence of a glycerol moiety, triacylglycerides and phospholipids (Forato *et al.*, 2000). The major difference between the ^1H -SPE-MAS spectra from drought-stressed and control lyophilised soybean leaves was the presence of a stronger peak at δ 1.62, which was assigned to the fatty acids present in the spectrum of the drought-stressed soybeans.

Data integration. The primary enzymes involved in the biosynthesis of the metabolites altered during water deficiency were identified from the KEGG database. The genes corresponding to these enzymes were identified by a subsequent search of the NCBI, Soykb and Phytozome databases. The expression of these genes in response to different water deficiency levels was assessed by analysing an RNA-seq library database derived from soybean leaves under water deficiency stress. Notably, since the soybean genome is highly duplicated (Schmutz *et al.*, 2010), multiple copies of the genes for all enzymes studied were identified.

As previously stated, water deficiency conditions affected the metabolite profile of soybean leaves mainly by leading to the biosynthesis of several amino acids, including isoleucine, leucine, valine, threonine, GABA, glutamate, proline, asparagine, tyrosine and phenylalanine (Fig. 3). Interestingly, of the enzyme-coding

genes related to these metabolites, at least one homologous gene was up-regulated in response to water deficiency (Figs S1 and S2).

Interestingly, according to the RNA-seq data, the genes coding for the enzymes involved in isoleucine, leucine, valine, proline, glutamate, asparagine and phenylalanine biosynthesis were expressed at higher levels in leaves, whereas the genes coding for enzymes involved in tyrosine (i.e. prephenate dehydrogenase and tyrosine aminotransferase) and aspartate (i.e. asparaginase) metabolism were expressed at higher levels in roots (Figs S1 and S2), exemplifying the differential expression of these genes in different tissues.

The observed changes in gene expression and compound abundance reflects the changes in plant metabolism in response to drought stress, including the production of solutes to maintain osmotic conditions and stabilise cellular structures (e.g. proline and other free amino acids) (Krasensky and Jonak, 2012).

During drought stress, a shortage of CO_2 assimilation coupled with changes in photosystem activities and the photosynthetic electron transport capacity results in the excess production of ROS. Proline protects membranes and proteins against oxidative stress and recruits antioxidants (Kocsy *et al.*, 2005; Molinari *et al.*, 2007). The peroxidase class of proteins is a group of enzymes involved in cell redox control. In our study, many copies of peroxidase genes were identified, and the gene expression data (RNA-seq) show that the expression of many of these genes were up-regulated in response to water deficiency (Figs S1 and S2).

ROS are produced and peroxidases are activated during water deficiency, but these components are also involved in cell wall synthesis and remodelling (Tenhaken, 2015). According to Tenhaken (2015), plants under drought stress conditions reduce shoot growth while maintaining root growth, requiring differential

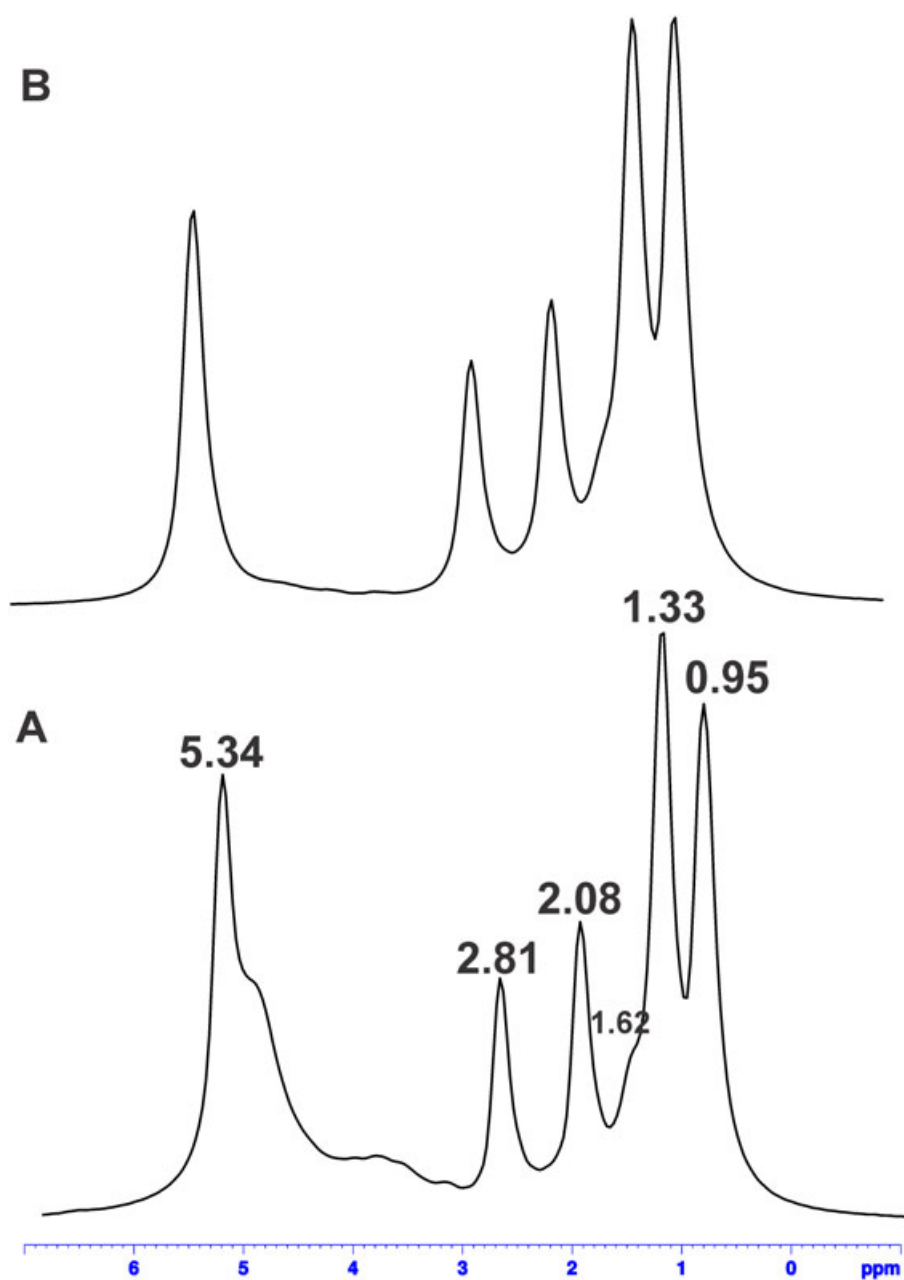


Figure 6. ^1H SPE-MAS profiles of lyophilised soybean leaves under water deficiency (A) and control (B) conditions. [Colour figure can be viewed at wileyonlinelibrary.com]

cell wall synthesis and remodelling. In this process, excess peroxidase activity, cross-linkable substrates and sufficient amounts of hydrogen peroxide (H_2O_2) favour the local stiffening of the wall, reducing cell wall expansion and thus strengthening the mechanical stability of the cells and organs. However, if H_2O_2 transiently accumulates in the presence of copper or iron in the cell wall, which are typically present in sufficient amounts, and the peroxidase activity or the substrate availability is limited, the formation of OH^\cdot radicals is favoured, causing the sugar polymers of the cell wall to be degraded and weakening the mechanical properties of the wall. Curiously, the expression of the peroxidase genes is more strongly induced in root tissue (Fig. S2) than in leaves (Fig. S1), which may be a consequence of differential cell wall synthesis and remodelling under drought stress conditions, in which plants reduce shoot growth while maintaining root growth.

Additionally, we detected a slight increase in the signals corresponding to glycoproteins, hemicellulose and cellulose in water-deficient samples in the analysis of the CP-MAS spectra of lyophilised soybean leaves, indicating changes in the cell wall components. Increased cellulose biosynthesis contributes to the maintenance of cell wall integrity and turgor pressure, allowing continuous cell growth under a low water potential (Gall *et al.*, 2015).

MapMan software was used to build metabolic maps based on the RNA-seq gene expression profiles obtained here to provide a global view of the major changes in the transcriptome profile of soybeans in response to water deficiency and to allow a better integration of the transcriptomic and NMR data. This technique allowed us to analyse the down- and up-regulated genes involved in the principal metabolic pathways in soybeans grown under

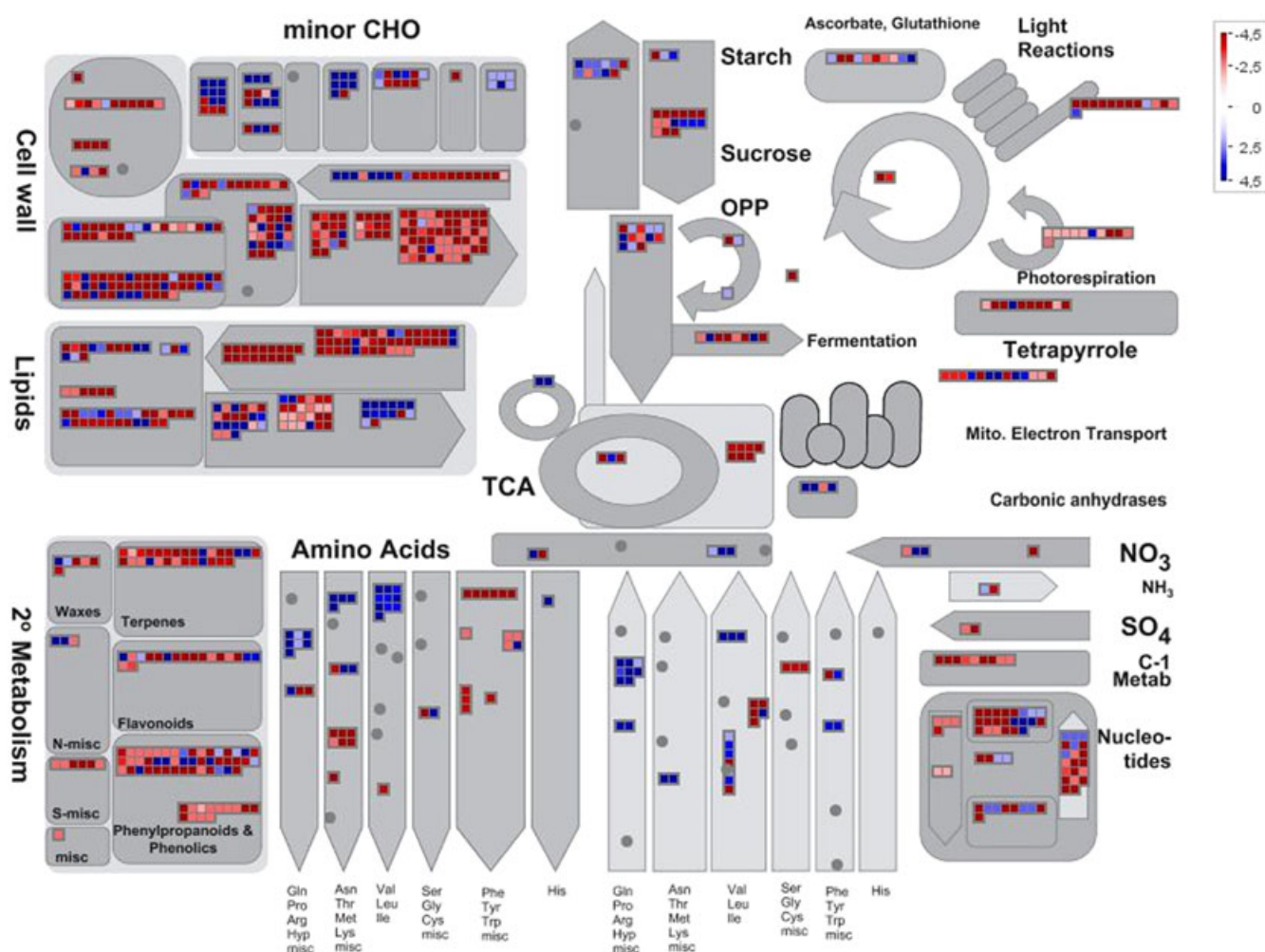


Figure 7. Metabolism overview in soybean leaf tissues upon water deficiency 3 (WD 3). Genes that were differentially expressed in response to WD 3 were mapped to specific functional categories (represented by squares) along the metabolism pathway by the MapMan software. The colour scale shows the log₂ fold change: red = up-regulated and blue = down-regulated. [Colour figure can be viewed at wileyonlinelibrary.com]

control and water deficiency conditions over time (Figs 7 and S5–S9). Interestingly, an increase in the expression of genes related to diverse metabolic pathways was observed in WD 3 (125 min + 150 min after stress) (Fig. 7), and most genes were related to amino acid metabolism, consistent with the metabolite changes indicated by the NMR analysis (Fig. 4).

As previously discussed, the NMR results identified alterations in amino acid and cell wall components in leaves under water deficiency. Consistent with these results, an overview of the metabolism (Figs 7 and S5–S9) showed that many genes related to amino acid and cell wall metabolism were differentially expressed in response to drought stress.

The overview of metabolism provided by MapMan also showed that several genes involved in lipid metabolism were differentially expressed, corroborating the analysis of the ¹H-SPE-MAS spectra that showed the presence of a stronger peak assigned to fatty acids in the spectrum of the drought-stressed soybeans than that of the control (Fig. 6). Lipids are important membrane components, and changes in their metabolism may preserve membrane integrity and cell compartmentation under water stress conditions. An analysis of gene expression in arabidopsis revealed that the expression of the primary lipid metabolism genes was altered in response to drought stress. In addition, an

increase in total lipid concentrations was previously observed in the leaves of tolerant grapevine genotypes during stress (Toumi *et al.*, 2008); moreover, a higher proportion and level of unsaturated fatty acids may be associated with leaf dehydration tolerance and post-drought recovery in bluegrass (Xu *et al.*, 2011). Additionally, plants, including soybeans, may also increase their drought tolerance by forming cuticular wax (of a lipidic nature) on their aerial surface, which mitigates water loss. The analysis of the soybean genome revealed the presence of 1127 genes related to lipid metabolism, 70 of which are involved in fatty acid elongation and wax and cutin metabolism (Schmutz *et al.*, 2010), highlighting the importance of this pathway.

In addition, the overview of metabolism indicates changes in glycolysis and the tricarboxylic acid (TCA) cycle, in which several genes are down- and up-regulated in response to drought stress (Figs 7 and S5–S9). The majority of the genes involved in the biosynthesis of secondary metabolites, particularly phenolic acids, were down-regulated or not differentially expressed, consistent with the ¹H HR-MAS spectra, which did not show significant differences in these metabolites in response to drought stress (Fig. 4).

The cellular response pathway generated by MapMan shows that different levels of drought stress altered cell development, cell

cycle/division, redox and the biotic and abiotic stress responses (Figs S7, S8, and S9). Under drought stress, developing cells are known to undergo transcriptomic reprogramming to adjust to the limited water conditions (Ma *et al.*, 2014; Osakabe *et al.*, 2014). As previously discussed, drought stress also interferes with the cell redox balance, mainly due to ROS production, which impacts cellular metabolism and cell wall and membrane integrity, resulting in the differential expression of several redox-related genes. Together with our physiological data (Fig. 1), the changes in the expression of the genes involved in the abiotic stress response confirms that stress was present and illustrates the activation of cellular defence mechanisms against drought stress. Interestingly, we also detected the differential expression of genes involved in biotic stress defence, showing the crosstalk between biotic and abiotic stress responses, probably due to the action of common signalling components, such as mitogen-activated protein kinases (MAPK) that trigger a cascade of signalling networks associated with the plant responses to both biotic and abiotic stress (Neupane *et al.*, 2013).

This study revealed the potential of integrating NMR-MAS and transcriptomic data. The ^1H HR-MAS parameters were optimised to permit the analysis of the samples without a broad signal from biomolecules or an effect of J-modulation distortions. Despite the low sensitivity of NMR-MAS techniques, the primary metabolites that were up-regulated by water deficiency were properly assigned in the ^1H HR-MAS spectrum, rigid and semi-rigid polysaccharides were readily observed using CP-MAS and mobile components were observed by SPE-MAS during the SSNMR analysis. In addition, multiple copies of the genes involved in the biosynthesis of the compounds affected by the water deficiency were identified in the soybean genome, and in many cases, several genes were up-regulated in response to the water deficiency conditions.

Therefore, our work has provided a complete picture of the major changes in the metabolic profile of soybeans in response to water deficiency. Drought stress enhances amino acid catabolism during water deficiency, which is a promising area for future studies on the regulation of water deficiency by metabolic signals. The information generated in this study may contribute to a better understanding of the molecular and phenotypic responses to drought stress and to the use of metabolite profiles as biomarkers for the selection of drought-tolerant genotypes in future studies.

Acknowledgements

This work was supported by the São Paulo Research Foundation (FAPESP), I.D.C. fellowship, process 2014/24006-0.

References

- André M, Dumez JN, Rezig L, Shintu L, Piotto M, Caldarelli S. 2004. Complete protocol for slow-spinning high resolution magic-angle spinning NMR analysis of fragile tissues. *Anal Chem* **86**: 10749–10754.
- Aguillar JA, Nilsson M, Bodenhausen G, Morris GA. 2012. Spin echo NMR spectra without J modulation. *Chem Commun* **48**: 811–813.
- Arbona V, Manzi M, Ollas C, Gómez-Cadenas A. 2013. Metabolomics as a tool to investigate abiotic stress tolerance in plants. *Int J Mol Sci* **14**: 4885–4911.
- Bowne JB, Erwin TA, Juttner J, Schnurbusch T, Langridge P, Bacic A, Roessner U. 2012. Drought responses of leaf tissues from wheat cultivars of differing drought tolerance at the metabolite level. *Mol Plant* **5**: 418–429.
- Carvalho AM, Bustamante MMC, Alcântara FA, Resck IS, Lemos SS. 2009. Characterization by solid-state CPMAS ^{13}C NMR spectroscopy of decomposing plant residues in conventional and no-tillage systems in central Brazil. *Soil Till Res* **102**: 144–150.
- Conte P, Pasquale C, Novotny EH, Caponetto G, Laudicina VA, Ciofalo M, Panno M, Palazzolo E, Badalucco L, Alonzo G. 2010. CPMAS ^{13}C NMR Characterization of leaves and litters from the reforested area of Mustigarufi in Sicily (Italy). *Open Magn Reson Rev* **3**: 89–95.
- Dick-Perez M, Zhang Y, Hayes J, Salazar A, Zabolina O, Hong M. 2011. Structure and interactions of plant cell-wall polysaccharides by two- and three-dimensional magic-angle-spinning solid-state NMR. *Biochemistry* **50**: 989–1000.
- Du H, Wang Z, Yu W, Huang B. 2012. Metabolic responses of hybrid bermudagrass to short-term and long-term drought stress. *J Am Soc Hortic Sci* **137**: 411–420.
- Emvas AM, Salek RM, Griffin JL, Merzaban J. 2013. NMR-based metabolomics in human disease diagnosis: Applications, limitations, and recommendations. *Metabolomics* **9**: 1048–1072.
- Fehr WR, Caviness CF, Burmood DT, Pennington JS. 1971. Stage of development descriptions for soybeans, *Glycine max* (L.) Merrill. *Crop Sci* **11**: 929–931.
- Ferreira LC, Neiverth W, Maronezzi LFF, Sibaldelli RNR, Nepomuceno AL, Farias JRB, Neumaier N. 2015. Efficiency of cover materials in preventing evaporation in drought-stressed soybeans grown in pots. *Revista de Ciências Agrárias: Amazonian J Agric and Enviro Sci* **58**: 349–356.
- Flexas J, Bota J, Loreto F, Cornic G, Sharkey TD. 2004. Diffusive and metabolic limitations to photosynthesis under drought and salinity in C3 plants. *Plant Biol* **6**: 269–279.
- Forato L, Colnago LA, Garratt RC, Lopes MA. 2000. Identification of free fatty acids in maize protein bodies and purified α zeins by ^{13}C and ^1H nuclear magnetic resonance. *Biochim Biophys Acta* **1543**: 106–114.
- Foston M. 2014. Advances in solid-state NMR of cellulose. *Curr Opin Biotechnol* **27**: 176–184.
- Gall HL, Philippe F, Domon JM, Gillet F, Pelloux J, Rayon C. 2015. Cell wall metabolism in response to abiotic stress. *Plants* **4**: 112–116.
- Hatcher PG. 1987. Chemical structural studies of natural lignin by dipolar dephasing solid state ^{13}C nuclear magnetic resonance. *Org Geochem* **11**: 31–39.
- Hoagland DR, Arnon DI. 1950. The water-culture method for growing for plants without soil. *Agric Exp Stn Circ* **347**: 1–32.
- Hochberg U, Degu A, Toubiana D, Gendler T, Nikolozki Z, Rachmilevitch S, Fait A. 2013. Metabolite profiling and network analysis reveal coordinated changes in grapevine water stress response. *BMC Plant Biol* **13**: 184.
- Iulianelli GCV, Tavares MI. 2016. Application of solid-state NMR spectroscopy to evaluate cassava genotypes. *J Food Comp Anal* **48**: 88–94.
- Knicker H, Lüdemann HD. 1995. N-15 and C-13 CPMAS and solution NMR studies of N-15 enriched plant material during 600 days of microbial degradation. *Org Geochem* **23**: 329–341.
- Krasensky J, Jonak C. 2012. Drought, salt, and temperature stress-induced metabolic rearrangements and regulatory networks. *J Exp Bot* **63**: 1593–1608.
- Kocsy G, Laurie R, Szalai G, Szilagyi V, Simon-Sarkadi L, Galiba G, de Ronde J. 2005. Genetic manipulation of proline levels affects antioxidants in soybean subjected to simultaneous drought and heat stresses. *Physiol Plant* **124**: 227–235.
- Laghi L, Picone G, Capozzi F. 2014. Nuclear magnetic resonance for foodomics beyond food analysis. *Trends Anal Chem* **59**: 93–102.
- Lanzinger A, Frank T, Reichenberger G, Herz M, Engel KH. 2015. Metabolite profiling of barley grain subjected to induced drought stress: responses of free amino acids in differently adapted cultivars. *J Agric Food Chem* **63**: 4252–4261.
- Lemma B, Nilsson I, Kleja DB, Olsson M, Knicker H. 2007. Decomposition and substrate quality of leaf litters and fine roots from three exotic plantations and a native forest in the southwestern highlands of Ethiopia. *Soil Biol Biochem* **39**: 2317–2328.
- Li H, Durbin R. 2009. Fast and accurate short-read alignment with Burrows-Wheeler transform. *Bioinformatics* **25**: 1754–1760.
- Ma X, Sukiran NL, Ma H, Su Z. 2014. Moderate drought causes dramatic floral transcriptomic reprogramming to ensure successful reproductive development in Arabidopsis. *BMC Plant Biol* **14**: 164.
- Manter DK, Kelsey RG. 2008. Ethanol accumulation in drought-stressed conifer seedlings. *Int J Plant Sci* **169**: 361–369.
- Melcher K, Ng LM, Zhou XE, Soon F, Xu Y, Suino-Powell KM, Park SY, Weiner JJ, Fujii H, Chinnusamy V, Kovach A, Li J, Wang Y, Li J, Peterson FC,

- Jensen DR, Yong EL, Volkman BF, Cutler SR, Zhu JK, Xu HE. 2009. A gate-latch-lock mechanism for hormone signalling by abscisic acid receptors. *Nature* **462**: 602–608.
- Molinari HBC, Marur CJ, Daros E, de Campos MKF, de Carvalho JFRP, Filho JCB, Pereira LFP, Vieira LGE. 2007. Evaluation of the stress-inducible production of proline in transgenic sugarcane (*Saccharum* spp.): Osmotic adjustment, chlorophyll fluorescence and oxidative stress. *Physiol Plant* **130**: 218–229.
- Neupane A, Nepal MP, Piya S, Subramanian S, Rohila JS, Reese RN, Benson BV. 2013. Identification, nomenclature, and evolutionary relationships of mitogen-activated protein kinase (MAPK) genes in soybean. *Evol Bioinforma* **9**: 363–386.
- Oliveira A, Martinelli CB, Lião LM, Pereira FC, Silveira-Lacerda EP, Alcantara GB. 2014. ¹H HR-MAS NMR and S180 cells: Metabolite assignment and evaluation of pulse sequence. *J Braz Chem Soc* **25**: 1135–1142.
- Osakabe Y, Osakabe K, Shinozaki K, Tran LSP. 2014. Response of plants to water stress. *Front Plant Sci* **5**: 86.
- Ramanlingam A, Kudapa H, Pazhamala LT, Weckwerth W, Varshney RK. 2015. Proteomics and metabolomics: Two emerging areas for legume improvement. *Front Plant Sci* **6**: 1–21.
- Rodrigues FA, Marcolino-Gomes J, Carvalho JFC, Nascimento LC, Neumaier N, Farias JBR, Carazzolle MF, Marcelino FC, Nepomuceno AL. 2012. Subtractive libraries for prospecting differentially expressed genes in the soybean under water deficit. *Genet Mol Biol* **35**: 304–314.
- Rodrigues FA, Fuganti-Pagliarini R, Marcolino-Gomes J, Nakayama TJ, Molinari HBC, Lobo FP, Harmon FG, Nepomuceno AL. 2015. Daytime soybean transcriptome fluctuations during water deficit stress. *BMC Genomics* **16**: 505.
- Santos ADC, Fonseca FA, Lião LM, Alcantara GB, Barison A. 2015. High-resolution magic angle spinning nuclear magnetic resonance in foodstuff analysis. *Trends Anal Chem* **73**: 10–18.
- Schmutz J, Cannon SB, Schlueter J, Ma J, Mitros T, Nelson W et al. 2010. Genome sequence of the palaeopolyploid soybean. *Nature* **463**: 178–183.
- Serra O, Chatterjee S, Huang W, Stark RE. 2012. Mini-review: What nuclear magnetic resonance can tell us about protective tissues. *Plant Sci* **195**: 120–124.
- Silvente S, Sovolev AP, Lara M. 2012. Metabolite adjustments in drought tolerant and sensitive soybean genotypes in response to water stress. *PLoS One* **7**: 1–11.
- Tenhaken R. 2015. Cell wall remodeling under abiotic stress. *Front Plant Sci* **5**: 1–9.
- Thimm O, Blasing O, Gibon Y, Nagel A, Meyer S, Kruger P, Selbig J, Muller LA, Rhee ASY, Stitt M. 2004. Mapman: a user-driven tool to display genomics data sets onto diagrams of metabolic pathways and other biological processes. *Plant J* **37**: 914–939.
- Toumi I, Gargouri M, Nouairi I, Moschou PN, Salem-Fnayou AB, Mliki A, Zarrouk M, Ghorbel A. 2008. Water stress induced changes in the leaf lipid composition of four grapevine genotypes with different drought tolerance. *Biol Plant* **52**: 161–164.
- Usadel B, Poree F, Nagel A, Lohse M, Czedik-Eysenberg A, Stitt M. 2009. A guide to using MapMan to visualize and compare Omics data in plants: A case study in the crop species, Maize. *Plant Cell Environ* **32**: 1211–1229.
- Uzilday B, Turkan I, Sekmen H, Ozgur R, Karakaya HC. 2012. Comparison of ROS formation and antioxidant enzymes in *Cleome gynandra* (C₄) and *Cleome spinosa* (C₃) under drought stress. *Plant Sci* **182**: 59–70.
- Verslues PE, Sharma S. 2010. Proline metabolism and its implications for plant–environment interaction. *Arabidopsis Book* **8**: e0140.
- Xu L, Han L, Huang B. 2011. Membrane fatty acid composition and saturation levels associated with leaf dehydration tolerance and post-drought rehydration in Kentucky bluegrass. *Crop Sci* **51**: 273–281.

Supporting information

Additional Supporting Information may be found online in the supporting information tab for this article.